

# Optical trapping using ultrashort 12.9fs pulses

Janelle Shane<sup>a</sup>, Michael Mazilu<sup>a</sup>, Woei Ming Lee<sup>a</sup>, and Kishan Dholakia<sup>a</sup>

<sup>a</sup>School of Physics and Astronomy, University of St Andrews, St Andrews, Fife, Scotland, United Kingdom

## ABSTRACT

We demonstrate stable three-dimensional optical trapping of 780nm silica particles using a dispersion-compensated 12.9fs infrared pulsed laser and a trapping microscope system with 1.40NA objective. To achieve these pulse durations we use the Multiphoton Intrapulse Interference Phase Scan (MIIPS) method to compensate for the significant temporal dispersion introduced by the trapping system. We demonstrate orders of magnitude reduction in pulse duration at the sample, and a dramatic increase in the efficiency of multiphoton excitation at the sample. The use of dispersion-compensated ultrashort pulses will therefore be a valuable tool for enhancing nonlinear processes in optically trapped particles. In addition, ultrashort pulses can allow the use of pulse shaping to control these nonlinear processes, yielding the possibility of advanced applications using coherent control of trapped particles.

**Keywords:** Optical trapping, optical tweezers, pulsed laser, femtosecond, ultrashort, dispersion compensation, pulse shaping, MIIPS

## 1. INTRODUCTION

Optical tweezing<sup>1,2</sup> has proven to be a valuable method for studying the properties of individual particles, cells, proteins, and more. Most optical tweezing is carried out with continuous-wave (CW) lasers, which have proven extremely successful for studying a variety of processes in optically trapped particles. However, researchers are increasingly exploring the use of pulsed lasers for optical tweezing, instead of and in addition to traditional CW sources. Pulsed lasers offer extremely high peak powers at lower average powers, allowing efficient access to multiphoton processes that would otherwise require enormously high average powers.

Previous research in pulsed optical tweezing has demonstrated some of these multiphoton processes in optically trapped particles. Using a CW trapping beam in combination with a pulsed nanosecond laser, Misawa and co-workers observed multiphoton ablation and self-focusing in trapped latex spheres.<sup>3</sup> Using pulsed femtosecond lasers as the trapping beam, Malmqvist and co-workers studied second harmonic generation (SHG) in optically trapped Rayleigh-sized KTP and LiNbO<sub>2</sub> particles,<sup>4</sup> while Agate and co-workers studied two-photon excitation in optically trapped dyed polymer particles in the Mie and Lorentz-Mie regime.<sup>5</sup> Perevedentseva and co-workers observed SHG in biotin and biotin ester microcrystals trapped by a pulsed laser.<sup>6</sup> Researchers have also used two-photon excitation in fluorescein medium surrounding optically trapped particles to study optical binding.<sup>7,8</sup> Morrish and co-workers have studied morphology-dependent resonances induced by two-photon excitation in optically trapped particles.<sup>9,10</sup> Fontes and co-workers studied two-photon morphology-dependent resonances, hyper-Raman, hyper-Rayleigh, and two-photon excitation in trapped particles (as well as linear effects).<sup>11</sup> Coherent anti-Stokes Raman scattering in trapped particles was studied by Chan and co-workers.<sup>12</sup> Kuriakose and co-workers studied two-photon morphology-dependent resonances in particles trapped by a femtosecond near-field optical traps.<sup>13</sup> Other research has explored the linear effects of pulsed lasers on trapped particles.<sup>14-18</sup>

The efficiency of these multiphoton processes depends on peak power. The ratio of peak power to average power is inversely related to pulse duration, so the shorter the pulse, the more multiphoton effects are seen at a given average power. These effects become dramatic as pulse duration drops below 100fs (Figure 1); however, the use of these pulse durations in optical trapping has remained almost completely unexplored. The examples given in the paragraph above use pulse durations of around 100fs and higher.

---

Send correspondence to K.D.: kd1@st-andrews.ac.uk.

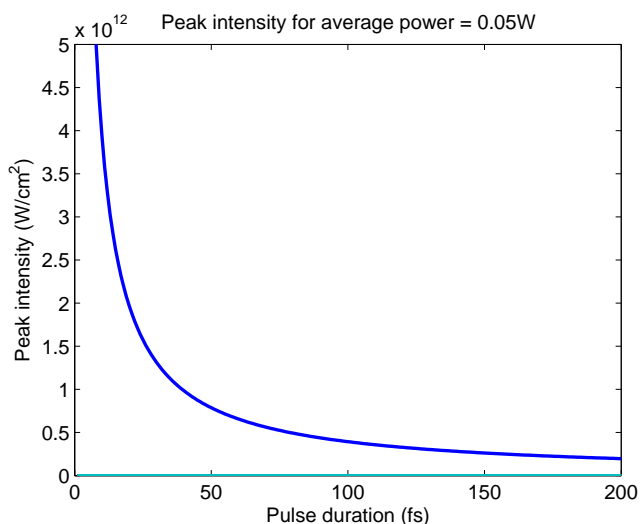


Figure 1. Peak intensity vs pulse duration for an 80MHz pulsed laser source of 50mW average power, focused to a spot of 1.1 micrometer diameter.

This paper will focus on the use of ultrashort pulsed lasers for optical trapping, beginning with an overview of dispersion in optical trapping systems and methods for dispersion pre-compensation, and demonstrating successful optical trapping of silica particles using a dispersion-compensated 12.9fs laser pulse. Definitions of “ultrashort” differ, but the term here refers to durations below 50fs full width at half maximum (FWHM), in contrast to the 100fs and longer durations more commonly used. At these durations, the laser’s bandwidth increases from a nanometer or two to tens or even hundreds of nanometers, and begins to play a very noticeable role in the way the laser interacts with materials. Peak power also increases dramatically compared to a 100fs pulse at the same average power, becoming orders of magnitude higher (Figure 1). Multiphoton effects such as two-photon excitation and second harmonic generation therefore increase dramatically in efficiency, allowing lower average powers to be used. Accordingly, detrimental effects such as photobleaching and thermal damage are reduced.<sup>19</sup> The broad bandwidth of ultrashort pulses also offers possibilities for shaping the spectral phase of the laser, leading to advanced applications such as low-background single-beam coherent anti-Stokes Raman scattering (CARS),<sup>20</sup> highly accurate refractive index measurement,<sup>21,22</sup> precise measurement of two-photon excitation spectra,<sup>23</sup> and selective multiphoton excitation without wavelength tuning or filters.<sup>24</sup>

Despite their advantages of increased peak power and bandwidth, ultrashort ( $\leq 50$ fs) pulses have not been used in optical trapping to date. The reason is not the availability of ultrashort lasers – turnkey systems with durations below 50fs have been commercially available for years. Currently, it is possible to buy ultrashort pulsed lasers with durations as low as 10fs. The price of these systems has been decreasing, and their reliability increasing. The primary reason these lasers have not found widespread use is the problem of temporal dispersion. Although spatial dispersion is also a factor due to the large bandwidth of these pulses, it is less of a problem and correctable using apochromatic optics,<sup>25</sup> and is not discussed here.

Temporal dispersion is an effect by which ultrashort pulses are stretched as they travel through microscope systems, particularly through high numerical aperture (NA) objectives. By the time they reach the sample, ultrashort pulses can be stretched by orders of magnitude, with peak power (and therefore multiphoton excitation efficiency) accordingly reduced. This happens because of the broadband nature of an ultrashort light pulse – the refractive index in materials is wavelength dependent, so some wavelengths travel faster through the microscope system than others. This creates a time lapse between the arrival of the faster and the slower wavelengths, lengthening the pulse and changing the wavelengths the sample sees as a function of time.

Although dispersive effects on 100fs and longer pulses are relatively subtle, even for microscope systems with plenty of glass and coatings, they become very significant for shorter pulses. This is due to the increased bandwidth of ultrashort pulses. Over a short wavelength range, the refractive index of most materials doesn’t

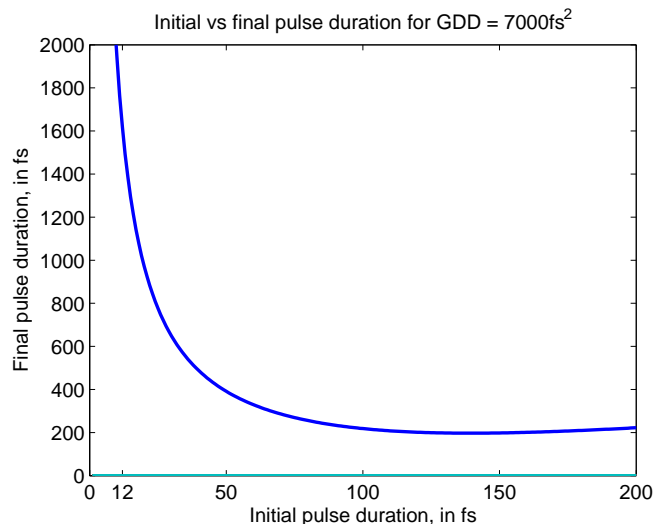


Figure 2. Calculated effect of dispersion on the FWHM duration of ultrashort pulses traveling through a typical microscope system. This calculation only considers GVD (2nd order distortions); microscope systems also have significant higher-order dispersion that further lengthens the pulse, as well as changing its temporal shape (making FWHM pulse duration less meaningful).

change very much, so there is not much difference between the arrival times of the fastest and slowest wavelengths within the narrow bandwidth of a 100fs pulse. However, a broadband ultrashort pulse can be dramatically stretched. In a typical microscope system, for example, a pulse that was originally 12fs can end up orders of magnitude longer at the sample than a pulse that was originally 120fs. This is illustrated by Figure 2, which shows the final durations of pulses with different initial durations, after traveling through a typical microscope system. Figure 2 was calculated using

$$\tau_f = \tau_i \sqrt{1 + \frac{16 \log(2)^2 \phi_2^2}{\tau_i^2}} \quad (1)$$

where  $\tau_f$  is the final FWHM (full width at half maximum) pulse duration,  $\tau_i$  is the initial transform-limited (TL) FWHM pulse duration, and  $\phi_2$  is the total 2nd order dispersion.<sup>26</sup> The total 2nd order dispersion  $\phi_2$  can be calculated for a given amount of material if the  $n''(\lambda)$  is known for the material:

$$\phi_2 = \frac{\lambda_0^3 c^2 n''(\lambda) l}{2\pi} \quad (2)$$

where  $\lambda_0$  is the wavelength of interest,  $c$  is the speed of light,  $n''(\lambda)$  is the 2nd derivative of the refractive index, and  $l$  is the length of the material that the pulse travels through.<sup>26</sup> Figure 2 uses a  $\phi_2$  of 7000 fs<sup>2</sup>, a typical figure for a microscope system with a high NA objective.<sup>25</sup>

Note that in the calculations for Figure 2, only 2nd order distortions are taken into account. Microscope systems also have significant higher-order dispersion that further lengthens the pulse, as well as changing its temporal shape. By the time they reach the sample, the pulses no longer have a Gaussian time profile, so FWHM pulse duration becomes a less meaningful measure of how much a pulse has been stretched. This paper will refer to the pulse durations of uncompensated pulses for convenience, but these numbers should be taken only as a rough indication of how much the pulses are stretched; FWHM pulse duration is still a relevant measure for TL pulses and for pulses stretched by 2nd order distortions only.

As the above discussion shows, the effects of dispersion are major obstacles that must be overcome if ultrashort pulses are to be used in microscope systems. Most strategies seek to measure or estimate the total dispersion in the system, then apply the opposite dispersion to the pulses so that the total dispersion is zero at the sample

plane. This general approach is called dispersion pre-compensation. Much of the challenge in dispersion pre-compensation lies in measuring the dispersion that must be compensated, with higher-order dispersion posing particular difficulty.

Several different approaches are commonly used for pre-compensating some or all of the dispersion in a microscope system. Some methods, such as prism pair<sup>27</sup> or grating pair<sup>28</sup> pre-compressors, can compensate for large amounts of 2nd order dispersion, but ignore or even worsen higher order dispersion. With 2nd order dispersion compensation only, combined with the introduced higher-order dispersion, it has been calculated that it is not possible to achieve pulses with less than 30fs pulse duration at the sample plane of a high-NA microscope, no matter how short the starting duration.<sup>25</sup> Chirped mirror pairs can be customized to completely compensate 2nd order and higher order dispersion,<sup>29,30</sup> but are relatively inflexible and cannot be adapted to frequently changing telescopes or microscope objectives, or to day-to-day variations in cavity dispersion. Pulse shapers are an extremely flexible, if more expensive, solution; they can produce almost any complex amount of dispersion, including higher orders.<sup>31</sup> These methods require dispersion measurement, whether by using a feedback signal such as second harmonic generation (SHG) to optimize the amount of dispersion compensated, or by use of an external dispersion measurement method such as SHG-FROG.<sup>32-34</sup>

In our experiments we use a method for combined dispersion measurement and precompensation, known as Multiphoton Intrapulse Interference Phase Scan (MIIPS).<sup>22,35,36</sup> The MIIPS method uses a pulse shaper to scan a reference phase function across the laser's spectrum. The effects of this reference phase function are monitored via second harmonic generation (SHG), usually generated in a nonlinear crystal placed at the sample plane. From the behavior of the second harmonic spectrum, the unknown dispersion present in the system can be directly calculated, and its inverse added to completely cancel out the dispersion. Because it is single-beam and non-interferometric, this method has been shown to adapt well to use in microscope systems;<sup>22</sup> here we report its first use in an optical trapping system.

## 2. EXPERIMENTAL SETUP

### 2.1 Optical trapping and trap stiffness measurement

The experiments presented here were carried out using a titanium sapphire oscillator (Femtolasers FemtoSource) capable of producing 12fs pulses centered at 800nm, at a repetition rate of 80MHz (the bandwidth that reached the sample was slightly narrower, capable of supporting 12.9fs pulses). Figure 3 shows the dispersion compensation and trapping setup. The beam was expanded by 2x and introduced into the pulse shaper, custom-built by BioPhotonic Solutions, Inc. The shaper includes a grating to spread the beam into its constituent frequencies, and a computer-controlled 640-pixel liquid crystal spatial light modulator (SLM) to modify the phase (and amplitude, not used in this work) of each of the beam's frequencies. The frequencies are recollected and recollimated via grating before leaving the shaper. For more details about this kind of shaper, see the review by Weiner.<sup>31</sup> After the shaper, the beam is expanded to overfill the back aperture of the objective used,<sup>37</sup> and sent to a homebuilt microscope which uses a 100x 1.40NA Nikon Plan Apo DIC H oil immersion objective. A quarter wave plate is used to circularly polarize the beam. The sample is illuminated from above by white light via a 40x 0.65NA Nikon 40x E Plan objective; this same objective collects transmitted laser light from the sample plane and sends it to quadrant photodiode (QPD) for position detection, as described below.

The position of a particle trapped at the laser focus is detected using back focal plane interferometry-based position sensing.<sup>38</sup> The interference pattern from the trapped microsphere is imaged onto a quadrant photodiode (QPD). The individual signals from each quadrant are amplified separately and converted to digital form using an NI USB-9162 data acquisition card. The position of the trapped particle is calculated from these four quadrant signals.

### 2.2 Dispersion measurement and compensation

As mentioned above, we use the MIIPS method for measuring and compensating the dispersion of our system. We repeat this measurement daily to adjust for day-to-day variations in cavity dispersion. This method requires the collection of second harmonic light generated by the laser at the sample plane, as shown by Figure 4. We generate this light using an 0.1mm thick BBO crystal, cut to be phase-matched for second harmonic generation

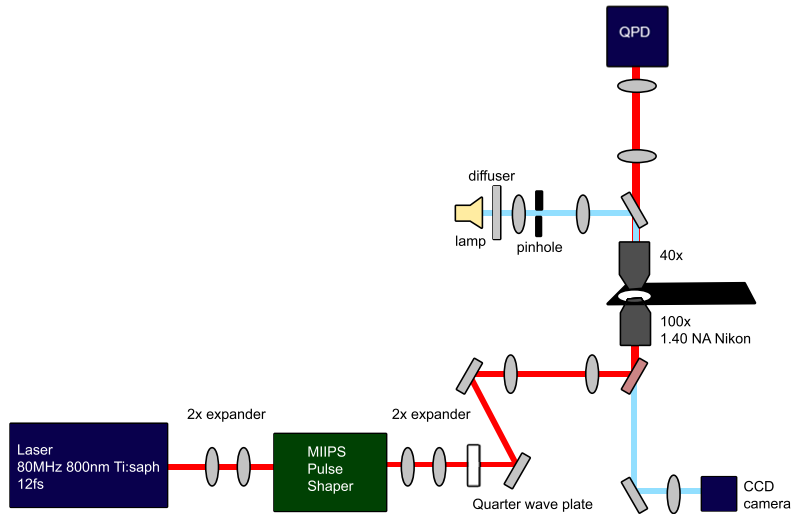


Figure 3. Experimental setup for ultrashort pulse optical trapping and position detection.

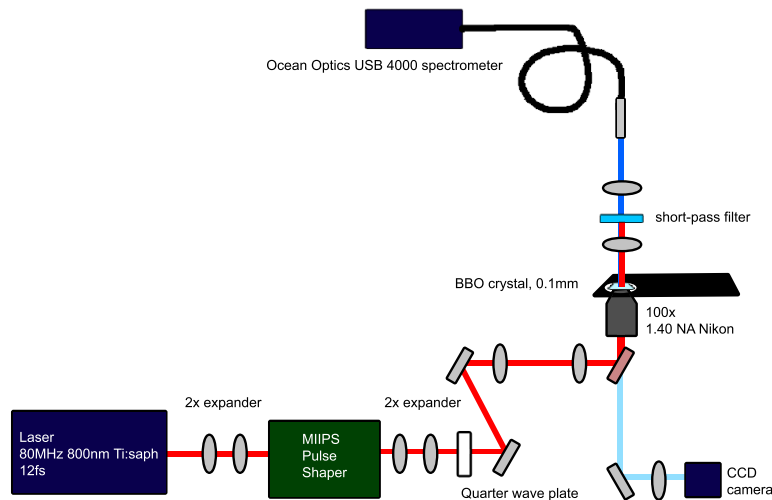


Figure 4. Experimental setup showing collection of second harmonic generation (SHG) light for use in the MIIPS dispersion measurement and compensation method. A thin (0.1mm) BBO crystal is placed in the sample plane, and a series of UV-grade fused silica lenses collects most of the SHG light, focusing it on the fiber head of the spectrometer.

at 800nm. The crystal is placed in the sample plane after immersion oil and a coverslip identical to those used for the microsphere samples. A quartz coverslip protects the top of the crystal; SHG light passes through the coverslip and is collected and focused on the fiber head of an Ocean Optics USB 4000 spectrometer. A short-pass filter normally prevents the laser's fundamental spectrum from reaching the spectrometer. To collect the laser's fundamental spectrum (needed for calculation of pulse duration at the sample), the short-pass filter is removed and white paper is used as an attenuating scatterer. When dispersion measurement is finished, we remove the SHG detection portion of the setup and replace it with the QPD position detection.

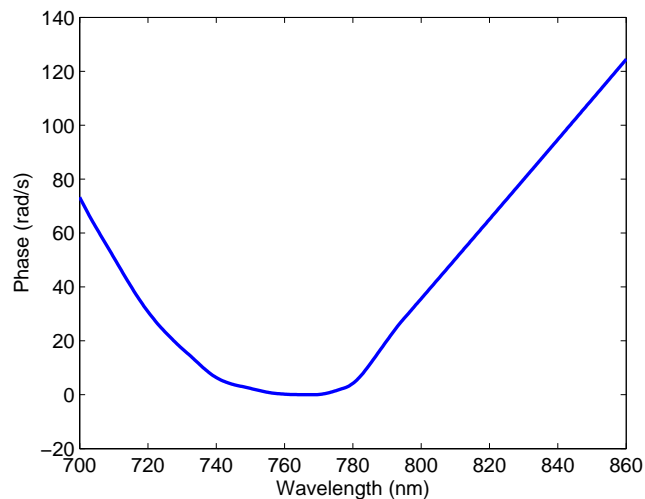


Figure 5. Total measured dispersion of the entire trapping system, including laser and pulse shaper. Note that although dispersion is dominated by a quadratic function (corresponding to GVD, or 2nd order dispersion), there is significant distortion of this curve, indicating the presence of higher-order dispersion as well. This measurement includes not only the trapping microscope but also residual dispersion in the laser cavity, and some slight dispersion introduced by the pulse shaper. It is also possible to calculate the dispersion of the trapping microscope alone, by measuring the dispersion of the system immediately after the MIIPS pulse shaper, and subtracting this from the measured total system dispersion.

### 3. RESULTS

#### 3.1 Dispersion compensation

Figure 5 shows the MIIPS measured dispersion of the entire optical trapping system, including the 100x oil immersion objective. This dispersion, expressed as phase delay as a function of wavelength, is dominated by a quadratic shape, indicating the presence of large amounts of 2nd order dispersion (also known as group velocity dispersion, or GVD). The dispersion contributed by BK7 glass (the vast majority of the dispersive material in the system) is known to be primarily second-order, so this finding comes as no surprise. The quadratic phase delay vs wavelength relationship, however, is modulated by additional distortions, indicating the presence of significant higher-order dispersion. BK7 glass does introduce small amounts of higher-order dispersion; antireflection coatings, dielectric mirrors, the laser cavity, and the shaper itself are also contributors of higher-order dispersion.

Once we measured dispersion, we were able to pre-compensate for it by using the shaper to add the inverse phase vs wavelength function. Note that because we measured higher orders of phase distortion, we were able to compensate these higher orders in addition to 2nd order phase distortion. It has been calculated that with 2nd order dispersion compensation only, the shortest possible pulse duration at the sample plane of a high NA microscope system is around 30fs.<sup>25</sup> By compensating all orders of dispersion we were able to obtain near transform-limited (TL) pulse durations of around 12.9fs FWHM. Some uncompensated residue does remain, particularly at spectral wings where generated SHG signal is weak, but the ratio of compensated pulse duration to theoretical TL pulse duration is less than 1.005.

The dispersion introduced by the microscope system has a dramatic effect on pulse duration at the sample. Figure 6 shows the calculated temporal profile of the pulse before (left) and after (right) dispersion compensation. These temporal profiles were calculated using inverse Fourier transform, given the laser's fundamental spectrum and measured spectral phase at the sample. The uncompensated pulse clearly shows the lengthening effects of 2nd order dispersion, as well as the temporally distorting effects of higher order dispersion. Because of these higher order dispersive effects, FWHM pulse duration (based on an assumed Gaussian temporal profile) becomes a less meaningful measure of pulse duration; however, it is evident that dispersion compensation has reduced pulse duration by roughly two orders of magnitude.

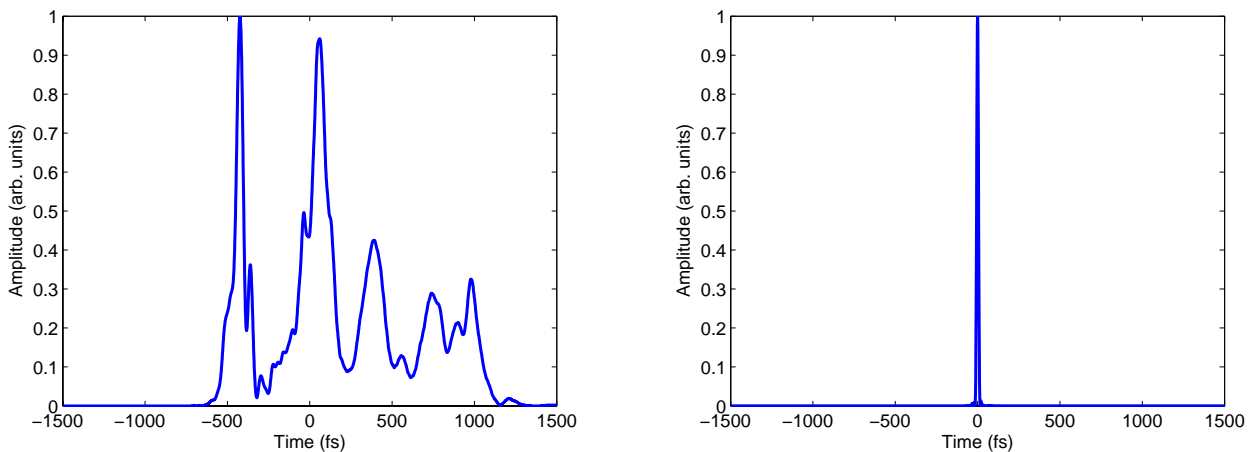


Figure 6. Calculated temporal profile of the pulse at the sample plane before (left) and after (right) dispersion compensation. These calculations were based on the pulse's measured spectral amplitude and phase, using inverse Fourier transform. The FWHM duration of the compensated pulse is 12.9 fs.

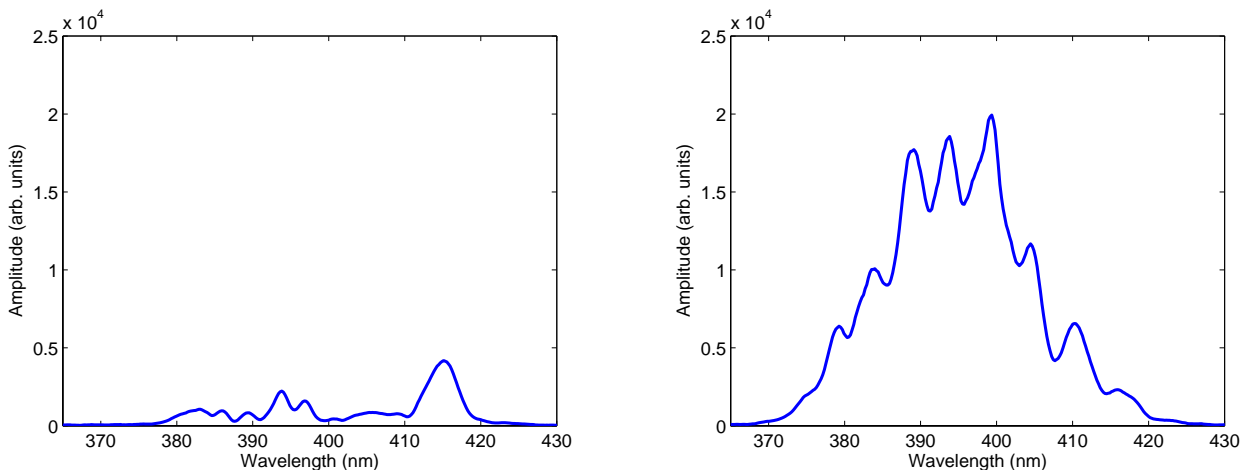


Figure 7. Second harmonic generated using a BBO crystal at the sample plane, before (left) and after (right) dispersion compensation. Note the difference in amplitude and shape.

The effects of this reduction of pulse duration (and therefore increase in peak power) on nonlinear processes can be clearly seen in Figure 7, which shows typical second harmonic signal generated in a BBO crystal by the laser beam before and after dispersion compensation. To increase the accuracy of compensation, the shaper's grating was translated to produce negative 2nd order dispersion; this had the effect of partially compensating for the positive 2nd order dispersion in the system and decreasing the amount of dispersion the shaper's SLM had to compensate. Without this additional precompensation, the SHG signal before MIIPS compensation would have been even weaker. The same average power was used in both cases, but dispersion compensation has increased the amount of second harmonic generation by about 740%. The uncompensated SHG signal changes from day to day, so dispersion compensation also increases reproducibility. A similar increase in efficiency and reproducibility can be expected for other multiphoton processes, such as two-photon excitation.

### 3.2 3D Optical trapping with 12.9fs pulses

To verify 3D optical trapping with our dispersion compensated 12.9fs pulses, we prepared a sample of 780nm diameter silica microspheres, diluted in deionized water. Silica was chosen as the trapping material because it

could withstand the dispersion-compensated peak powers at the average powers needed for trapping; polymer was violently ablated (an effect almost identical to that observed by Misawa and co-workers<sup>3</sup>) and gold caused cavitation.

We measured and compensated the trapping system's dispersion on the same day that these data were taken, to account for day-to-day dispersion fluctuations in the laser cavity (these fluctuations were enough to stretch the pulses by 50fs or more).

We trapped the silica particles at the focus of the laser beam, with an average power at the sample plane of 47mW, measured using the double-objective transmission method.<sup>39</sup> The sample was diluted enough that only a single particle was trapped at a time, which we confirmed by imaging the sample with a CCD camera (Figure 3). The trapping distance was 14 $\mu$ m from the bottom coverslip.

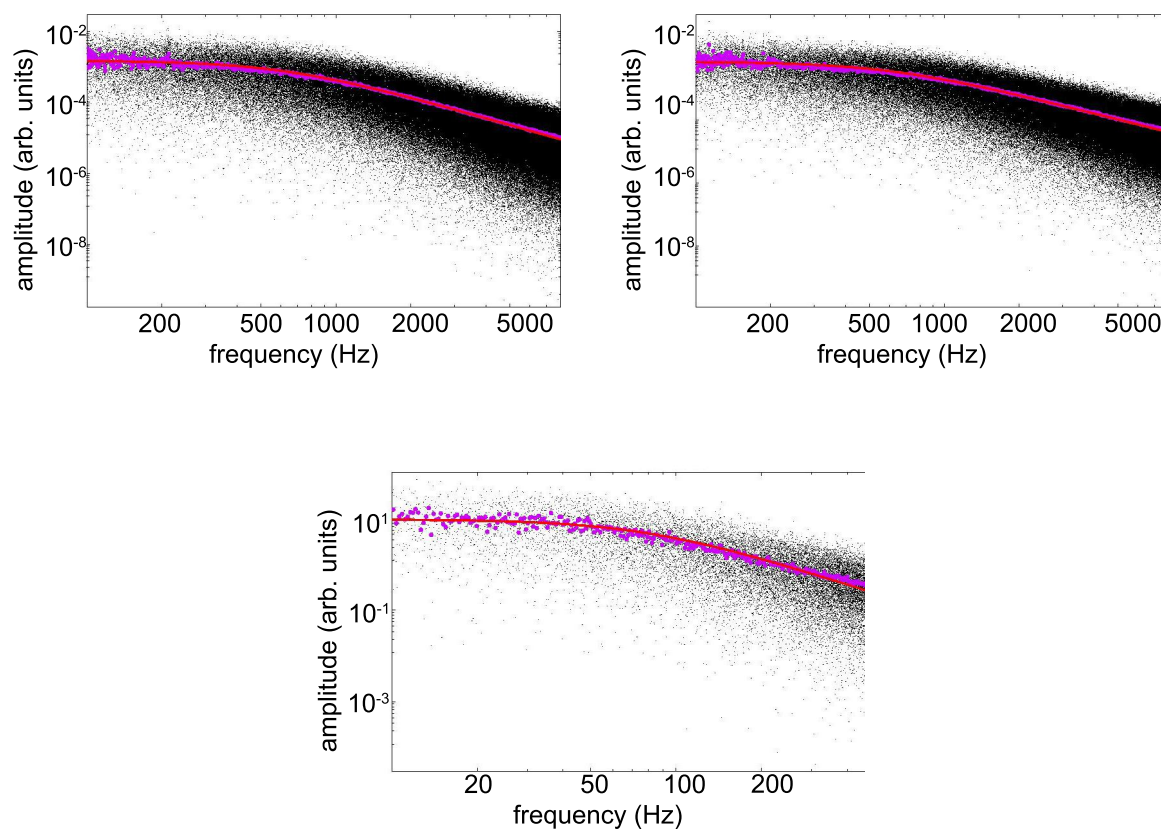


Figure 8. Power spectra of a trapped 780nm silica sphere in x, y, and z directions (upper left, upper right, and bottom, respectively). These power spectra were calculated from a 40 second acquisition at an acquisition rate of 30,000 samples/second. The particle was trapped with 47mW average power using dispersion-compensated 12.9fs pulses at 80MHz repetition rate. We fit Lorentzian curves to these power spectra; these fitted curves are shown superimposed on the experimental data. To equally weight the low and high frequencies when fitting, we chose a fitting range that would center the cutoff frequency along the frequency axis in log-log space. The x and y axes are fit from 100Hz - 8000Hz, while the z axis (with lower cutoff frequency) is fit from 10Hz - 500Hz.

The positions of the trapped silica particles were monitored over 6.7 consecutive seconds at an acquisition rate of 30,000 samples/second for each of the four quadrants of the QPD. This position measurement was repeated six consecutive times for each of three different silica particles (giving a total combined acquisition length of 40



seconds for each particle). We used our own Mathematica program to calculate the power spectra in x, y, and z of each 40 second acquisition and fit a Lorentzian curve to these power spectra. These power spectra and fit for one of the trapped silica particles is shown in Figure 8. The cutoff frequency of the fitted Lorentzian curve was then used to calculate the trap stiffness.<sup>38</sup>

The power spectra indicate stable trapping in 3D by the 12.9fs pulsed laser, which we visually confirmed by translating the sample stage in x, y, and z. We calculate an average trap stiffness of  $0.1094 \pm 0.009$  pN/nm in the x-direction,  $0.1204 \pm 0.008$  pN/nm in the y-direction, and  $0.0216 \pm 0.008$  pN/nm in the z-direction.

#### 4. CONCLUSION

In this work we have demonstrated stable optical trapping of 780nm silica particles using a dispersion-compensated 12.9fs pulsed laser. The use of these pulse durations at the sample required us to overcome the significant temporal dispersion introduced by the trapping system, in particular the 1.40NA 100x objective. We demonstrate that dispersion compensation decreases pulse duration at the sample by orders of magnitude and accordingly dramatically increases the efficiency of multiphoton excitation at the sample. The use of ultrashort pulses with dispersion compensation will therefore be a valuable tool for enhancing nonlinear processes in optically trapped particles. In addition, ultrashort pulses can allow the use of pulse shaping to control these nonlinear processes, yielding the possibility of applications such as low-background CARS<sup>20</sup> or selective two-photon excitation<sup>24</sup> in trapped particles.

#### 5. ACKNOWLEDGEMENTS

The authors thank the UK Engineering and Physical Sciences Research Council (EPSRC) for funding. MM acknowledges support from Scottish Enterprise. JS was supported in part by a USA National Science Foundation Graduate Research Fellowship.

#### REFERENCES

- [1] Ashkin, A., Dziedzic, J., Bjorkholm, J., and Chu, S., "Observation of a single-beam gradient force optical trap for dielectric particles," *Optics Letters* **11**(5), 288–290 (1986).
- [2] Ashkin, A., "Forces of a single-beam gradient laser trap on a dielectric sphere in the ray optics regime," *Biophys. J.* **61**(2), 569–582 (1992).
- [3] Misawa, H., Koshioka, M., Sasaki, K., Kitamura, N., and Masuhara, H., "Three-dimensional optical trapping and laser ablation of a single polymer latex particle in water," *Journal of Applied Physics* **70**, 3829 (1991).
- [4] Malmqvist, L. and Hertz, H. M., "2nd-harmonic generation in optically trapped nonlinear particles with pulsed lasers," *Applied Optics* **34**(18), 3392–3397 (1995).
- [5] Agate, B., Brown, C. T. A., Sibbett, W., and Dholakia, K., "Femtosecond optical tweezers for in-situ control of two-photon fluorescence," *Optics Express* **12**(13), 3011–3017 (2004).
- [6] Perevedentseva, E. V., Karmenyan, A. V., Kao, F. J., and Chiou, A., "Second harmonic generation of biotin and biotin ester microcrystals trapped in optical tweezers with a mode-locked Ti : Sapphire laser," *Scanning* **26**, I78–I82 (Sept. 2004).
- [7] Dholakia, K., Little, H., Brown, C. T. A., Agate, B., McGloin, D., Paterson, L., and Sibbett, W., "Imaging in optical micromanipulation using two-photon excitation," *New Journal of Physics* **6** (2004).
- [8] Metzger, N. K., Wright, E. M., Sibbett, W., and Dholakia, K., "Visualization of optical binding of microparticles using a femtosecond fiber optical trap," *Optics Express* **14**(8), 3677–3687 (2006).
- [9] Morrish, D., Gan, X. S., and Gu, M., "Morphology-dependent resonance induced by two-photon excitation in a micro-sphere trapped by a femtosecond pulsed laser," *Optics Express* **12**(18), 4198–4202 (2004).
- [10] Morrish, D., Gan, X. S., and Gu, M., "Scanning particle trapped optical microscopy based on two-photon-induced morphology-dependent resonance in a trapped microsphere," *Applied Physics Letters* **88**(14) (2006).
- [11] Fontes, A., Ajito, K., Neves, A. A. R., Moreira, W. L., de Thomaz, A. A., Barbosa, L. C., de Paula, A. M., and Cesar, C. L., "Raman, hyper-Raman, hyper-Rayleigh, two-photon luminescence and morphology-dependent resonance modes in a single optical tweezers system," *Physical Review E* **72**(1) (2005).

- [12] Chan, J. W., Winhold, H., Lane, S. M., and Huser, T., "Optical trapping and coherent anti-Stokes Raman scattering (CARS) spectroscopy of submicron-size particles," *IEEE Journal of Selected Topics in Quantum Electronics* **11**(4), 858–863 (2005).
- [13] Kuriakose, S., Morrish, D., Gan, X., Chon, J. W. M., Dholakia, K., and Gu, M., "Near-field optical trapping with an ultrashort pulsed laser beam," *Applied Physics Letters* **92**(8), 081108 (2008).
- [14] Ambardekar, A. A. and Li, Y. Q., "Optical levitation and manipulation of stuck particles with pulsed optical tweezers," *Optics Letters* **30**(14), 1797–1799 (2005).
- [15] Deng, J. L., Wei, Q., Wang, Y. Z., and Li, Y. Q., "Numerical modeling of optical levitation and trapping of the "stuck" particles with a pulsed optical tweezers," *Optics Express* **13**(10), 3673–3680 (2005).
- [16] Mao, F. L., Xing, Q. R., Wang, K., Lang, L. Y., Wang, Z., Chai, L., and Wang, Q. Y., "Optical trapping of red blood cells and two-photon excitation-based photodynamic study using a femtosecond laser," *Optics Communications* **256**(4-6), 358–363 (2005).
- [17] Wang, L. G. and Zhao, C. L., "Dynamic radiation force of a pulsed Gaussian beam acting on a Rayleigh dielectric sphere," *Optics Express* **15**(17), 10615–10621 (2007).
- [18] Pan, L. Y., Ishikawa, A., and Tamai, N., "Detection of optical trapping of CdTe quantum dots by two-photon-induced luminescence," *Physical Review B* **75**(16) (2007).
- [19] Xi, P., Andegeko, Y., Weisel, L. R., Lozovoy, V. V., and Dantus, M., "Greater signal, increased depth, and less photobleaching in two-photon microscopy with 10 fs pulses," *Optics Communications* **281**(7), 1841–1849 (2008).
- [20] Dudovich, N., Oron, D., and Silberberg, Y., "Single-pulse coherently controlled nonlinear Raman spectroscopy and microscopy," *Nature* **418**(6897), 512–514 (2002).
- [21] Coello, Y., Xu, B., Miller, T., Lozovoy, V., and Dantus, M., "Group-velocity dispersion measurements of water, seawater, and ocular components using Multiphoton Intrapulse Interference Phase Scan," *Applied Optics* **46**(35), 8394–8401 (2007).
- [22] Xu, B., Gunn, J. M., Cruz, J. M. D., Lozovoy, V. V., and Dantus, M., "Quantitative investigation of the Multiphoton Intrapulse Interference Phase Scan method for simultaneous phase measurement and compensation of femtosecond laser pulses," *Journal of the Optical Society of America B* **23**(4), 750–759 (2006).
- [23] Lozovoy, V., Xu, B., Shane, J., and Dantus, M., "Selective nonlinear optical excitation with pulses shaped by pseudorandom Galois fields," *Physical Review A* **74**(4), 41805 (2006).
- [24] Dela Cruz, J., Pastirk, I., Comstock, M., Lozovoy, V., and Dantus, M., "Use of coherent control methods through scattering biological tissue to achieve functional imaging," *Proceedings of the National Academy of Sciences, USA* **101**(49), 16996–7001 (2004).
- [25] Guild, J. B., Xu, C., and Webb, W. W., "Measurement of group delay dispersion of high numerical aperture objective lenses using two-photon excited fluorescence," *Journal of Applied Optics* **36**(1), 397–401 (1997).
- [26] Salin, F. and Brun, A., "Dispersion compensation for femtosecond pulses using high-index prisms," *Journal of Applied Physics* **61**(10), 4736–4739 (1987).
- [27] Fork, R. L. and Martinez, O. E., "Negative dispersion using pairs of prisms," *Optics Letters* **9**(5), 150 (1984).
- [28] Treacy, E., "Optical pulse compression with diffraction gratings," *Quantum Electronics, IEEE Journal of* **5**(9), 454–458 (1969). 0018-9197.
- [29] Szípcos, R., Ferencz, K., Spielmann, C., and Krausz, F., "Chirped multilayer coatings for broadband dispersion control in femtosecond lasers," *Optics Letters* **19**(3), 201 (1994).
- [30] Kaertner, F. X., Morgner, U., Ell, R., Schibli, T., Fujimoto, J. G., Ippen, E. P., Scheuer, V., Angelow, G., and Tschudi, T., "Ultrabroadband double-chirped mirror pairs for generation of octave spectra," *Journal of the Optical Society of America B* **18**(6), 882–885 (2001).
- [31] Weiner, A. M., "Femtosecond pulse shaping using spatial light modulators," *Review of Scientific Instruments* **71**(5), 1929–1960 (2000).
- [32] Amat-Roldán, I., Cormack, I., Loza-Alvarez, P., Gualda, E., and Artigas, D., "Ultrashort pulse characterisation with SHG collinear-FROG," *Optics Express* **12**(6), 1169–1178 (2004).
- [33] Fittinghoff, D. N., Squier, J. A., Barty, C. P. J., Sweetser, J. N., Trebino, R., and Mueller, M., "Collinear type II second-harmonic-generation frequency-resolved optical gating for use with high-numerical-aperture objectives," *Optics Letters* **23**(13), 1046–1048 (1998).

- [34] Amat-Roldán, I., Cormack, I. G., Loza-Alvarez, P., and Artigas, D., “Starch-based second-harmonic-generated collinear frequency-resolved optical gating pulse characterization at the focal plane of a high-numerical-aperture lens,” *Optics Letters* **29**(19), 2282–2284 (2004).
- [35] Lozovoy, V. V., Pastirk, I., and Dantus, M., “Multiphoton Intrapulse Interference. IV. ultrashort laserpulse spectral phase characterization and compensation,” *Optics Letters* **29**(7), 775–777 (2004).
- [36] Dantus, M., Lozovoy, V. V., and Pastirk, I., “MIIPS characterizes and corrects femtosecond pulses,” *Laser Focus World* **43**, 101–104 (2007).
- [37] Neuman, K. C. and Block, S. M., “Optical trapping,” *Review of Scientific Instruments* **75**(9), 2787–2809 (2004).
- [38] Gittes, F. and Schmidt, C. F., “Interference model for back-focal-plane displacement detection in optical tweezers,” *Optics Letters* **23**(1), 7–9 (1998).
- [39] Svoboda, K. and Block, S., “Biological applications of optical forces,” *Annual Reviews in Biophysics and Biomolecular Structure* **23**(1), 247–285 (1994).